Preprints.org

Article

Not peer-reviewed version

Sensor Placement Strategies for Target Localization via 3-D TOA Measurements in Underwater Acoustic Sensor Networks

Rongyan Zhou *, Weijie Tan, Meng Li, Baosheng Wang

Posted Date: 28 April 2026

doi: 10.20944/preprints202604.1929.v1

Keywords: time of arrival (TOA); underwater acoustic sensor networks (UASNs); Cramer-Rao lower bound (CRLB); optimal sensor placement; MinMax *k*-Means algorithm

Preprints.org is a free multidisciplinary platform providing preprint service that is dedicated to making early versions of research outputs permanently available and citable. Preprints posted at Preprints.org appear in Web of Science, Crossref, Google Scholar, Scilit, Europe PMC, OpenAlex.

Copyright: This open access article is published under a Creative Commons CC BY 4.0 license, which permit the free download, distribution, and reuse, provided that the author and preprint are cited in any reuse.

Preprints.org (www.preprints.org) | NOT PEER-REVIEWED | Posted: 28 April 2026 doi:10.20944/preprints202604.1929.v1

Disclaimer/Publisher's Note: The statements, opinions, and data contained in all publications are solely those of the individual author(s) and contributor(s) and not of MDPI and/or the editor(s). MDPI and/or the editor(s) disclaim responsibility for any injury to people or property resulting from any ideas, methods, instructions, or products referred to in the content.

Article

Sensor Placement Strategies for Target Localization via 3-D TOA Measurements in Underwater Acoustic Sensor Networks

Rongyan Zhou [1,*], Weijie Tan [2], Meng Li [1] and Baosheng Wang [1]

[1] School of Information Engineering, Nanyang Institute of Technology, Nanyang 473004, China
[2] State Key Laboratory of Public Big Data, Guizhou Big Data Academy, Guizhou University, Guiyang 550025, China
* Correspondence: zhoury@mail.nwpu.edu.cn

Abstract

This article investigates sensor placement strategies for three-dimensional (3-D) time-of-arrival (TOA)-based target localization in Underwater Acoustic Sensor Networks (UASNs). To mitigate underestimation of localization accuracy in complex marine environments, the actual acoustic ray propagation time is derived, and the TOA measurement variance is estimated using the ray acoustic propagation model. These formulations enable a novel 3-D TOA measurement model, and the trace of Cramér-Rao lower bound (CRLB) for this model serves as the optimization criterion for sensor placement. The MinMax k-Means algorithm is proposed to determine the optimal sensor placement by minimizing the average of the trace of CRLB. Extensive numerical simulations are conducted to demonstrate the effectiveness of the placement strategies.

Keywords: Time of arrival (TOA); Underwater Acoustic Sensor Networks (UASNs); Cramer-Rao lower bound (CRLB); optimal sensor placement; MinMax k-means algorithm

---

0. Introduction

Underwater Acoustic Sensor Networks (UASNs) have attracted considerable attention over the past few decades [1,2], driving the recent development of numerous potential applications, such as underwater security, ocean surveys, and submarine exploration [3,4]. Among various research topics in UASNs, target localization represents a fundamental capability, typically achieved by acquiring time, angle, and received signal strength measurements and executing corresponding localization algorithms [5–7].

Several localization techniques have been developed for UASNs, including time of arrival (TOA) and time difference of arrival (TDOA) methods, angle of arrival (AOA) techniques based on angle measurement, and received signal strength (RSS) based on signal energy measurement [8–10]. Among these, TOA-based localization offers several distinct advantages in underwater environments, making it the preferred choice for many underwater localization applications [11]. In recent years, extensive research has been conducted to improve the target localization accuracy in UASNs. Existing approaches can be broadly categorized into two groups: improving localization algorithms and optimizing sensor placement strategies. However, the majority of studies have focused on localization algorithms [12,13], while relatively few works have addressed sensor placement strategies. Given the complexity of underwater acoustic propagation, it is essential to incorporate the complex underwater acoustic channel characteristics when optimizing sensor placement [14,15]. Therefore, determining the optimal sensor placement in UASNs has become a critical research problem.

To address this challenge, the Cramér-Rao Lower Bound (CRLB) has been widely adopted as a performance metric for sensor placement optimization. The CRLB is the inverse of the Fisher information matrix (FIM), characterizes the theoretical lower bound on localization estimation variance. Achieving the CRLB indicates that an estimator has attained the optimal localization performance. Consequently,

© 2026 by the author(s). Distributed under a Creative Commons CC BY license.

Preprints.org (www.preprints.org) | NOT PEER-REVIEWED | Posted: 28 April 2026 doi:10.20944/preprints202604.1929.v1

CRLB-based criteria are commonly employed to formulate sensor placement optimization problems [16–18]. In two-dimensional (2-D) space, the optimal sensor-target geometry for multistatic TOA localization was derived in [19], where the optimality criterion minimizes the area of the estimation confidence region, equivalent to maximizing the determinant of the FIM(D-optimality). Extending to three-dimensional (3-D) scenarios, a novel optimization framework was formulated by minimizing the trace of CRLB with TOA measurement in 3-D space [20]. Furthermore, the concepts of maximum feasible angle and separation angle were introduced in [21] to transform the objective function and constraints into equivalent angular forms, maximizing the determinant of the FIM to optimize range sensor placement in constrained regions. More recently, the authors in [22] propose an efficient block majorization-minimization algorithm for optimal 3-D sensor placement with closed-form solutions and guaranteed convergence.

Although the aforementioned works provide many optimal sensor placement strategies, the existing optimization frameworks can not be directly applied to sensor placement problem in UASNs. In general, the underwater acoustic measurement models are inherently complex, influenced by factors such as the acoustic velocity profiles and the multipath effects [24]. In [25] proposed an optimal sensor placement method for 3-D underwater target localization using range-only measurements. However, the optimization process relied on idealized acoustic propagation models (e.g., constant sound speed), potentially reducing robustness in real underwater scenarios. To address this limition, a multivariate nonlinear optimization problem was formulated in [26] to minimize the trace of CRLB with a practical isogradient sound speed profile (SSP). Nevertheless, the resulting optimization problem was nonconvex and multivariate, preventing guarantees of global optimality. Later, to enhance practicality, the effects of SSP and the active sonar equation were integrated in [27] to improve coverage calculations and localization performance. However, the recommended star five-node placement method was costly and impractical for large-scale implementation. More recently, Huang [28] adopted the criterion of minimizing the trace of the CRLB to determine the optimal placement of reference nodes under Gaussian measurement noise, which correlates with the signal propagation path in 3-D underwater space. However, the computational complexity and adaptability to large-scale or heterogeneous underwater networks remained unverified.

In respond to the aforementioned limitations, this paper focuses on optimal sensor placement for 3-D TOA-based target localization in UASNs. The main contributions of this work are summarized as follows:

- A novel 3-D TOA measurement model is developed that incorporates the actual acoustic ray popagation time and TOA measurement variance estimated using a ray acoustic propagation model.
- The CRLB for the proposed 3-D TOA estimation methods is derived, with the trace of CRLB serving as the optimization criterion for sensor placement, providing a theoretical foundation for performance evaluation.
- A CRLB-based MinMax *k*-Means optimization algorithm is proposed to determine the optimal sensor placement problem by minimizing the average of the trace of CRLB, ensuring guaranteed convergence with reduced computational complexity compared to existing nonconvex optimization methods.
- Extensive simulation results validate the theoretical analysis, demonstrating that the proposed optimal sensor placement strategies achieve superior localization accuracy compared to existing placement schemes under the same parameter settings.

The remainder of this paper is organized as follows: Section 1 presents the 3-D TOA-based localization measurement model and formulates the sensor placement optimization problem. Section 2 develops the CRLB-based MinMax *k*-Means optimization algorithm to solve the sensor placement problem. Section 3 provides extensive numerical simulations to validate the theoretical analysis and evaluate the performance of the proposed placement strategies. Finally, Section 4 concludes the paper and discusses future research directions.

© 2026 by the author(s). Distributed under a Creative Commons CC BY license.

Preprints.org (www.preprints.org) | NOT PEER-REVIEWED | Posted: 28 April 2026 doi:10.20944/preprints202604.1929.v1

1. System Model and Problem Formulation

In this section, we first introduce the TOA-based 3-D localization measurement model and the involved parameters. Subsequently, we adopt the isogradient sound speed profile and varied noise measurement to quantify the localization error in terms of the CRLB.

1.1. System Scenario

In this paper, we consider a 3-D underwater acoustic localization scenario, where a stationary target is to be located using N cooperative sensors. Let $\mathcal{C} = \{1, 2, 3, \ldots, N\}$ denote the set of sensors, $\mathbf{q} = [x, y, z]^\intercal \in \mathbb{R}^3$ represent the position of the target, and $\mathbf{p}_i = [x_i, y_i, z_i]^\intercal$ denote the location of the ith sensor, where $i \in \mathcal{C}$. The distance between the target and the ith sensor is given by $r_i = \|\mathbf{q} - \mathbf{p}_i\|$, where $\| \cdot \|$ denotes the Euclidean norm. Assuming that the acoustic signal generated at time t_0 arrives at sensor $\mathbf{p}_i$ at time is t_i, and the signal propagation speed is c. The signal arrival time of the ith sensor in a noisy environment can be expressed as

$$t_i = t_0 + \frac{r_i}{c} + \chi_i = t_0 + \hat{t}_i + \chi_i \tag{1}$$

Here χ_i denotes the measurement noise, which is assumed to be mutually independent and follows a zero-mean Gaussian distribution with variance σ_i^2. The measurement noise covariance matrix can be expressed as a diagonal matrix given by

$$\mathbf{Q} = \mathrm{cov}\left(\chi\chi^{\mathrm{T}}\right) = \mathrm{diag}\left(\sigma_1^2, \sigma_2^2, \cdots, \sigma_N^2\right) \tag{2}$$

In order to facilitate the analysis, we assumed that the signal occurrence time $t_0 = 0$. Based on this assumption, the vector form of the measurement model can be expressed as

$$\mathbf{t} = \hat{\mathbf{t}} + \chi \tag{3}$$

with

$$\begin{aligned} \mathbf{t} &= \begin{bmatrix} t_1 & t_2 & \cdots & t_N \end{bmatrix}^{\mathrm{T}} \\ \hat{\mathbf{t}} &= \begin{bmatrix} \hat{t}_1 & \hat{t}_2 & \cdots & \hat{t}_N \end{bmatrix}^{\mathrm{T}} \\ \chi &= \begin{bmatrix} \chi_1 & \chi_2 & \cdots & \chi_N \end{bmatrix}^{\mathrm{T}} \end{aligned} \tag{4}$$

The underwater sound speed is a hierarchical variable. Generally, it follows an isogradient depth-dependent SSP and can be expressed as

$$c(z) = b + az \tag{5}$$

where b is the sound speed at the sea surface, and a denotes the steepness of the SSP. Meanwhile, the target signal fails to satisfy the isotropic conditions, and the actual acoustic path does not propagate along a straight line but follows a curved trajectory [29]. The deflection angle of the actual acoustic path relative to the straight line connecting the target and the ith sensor is derived from Snell's law and can be expressed as

$$\alpha_i = \arctan \frac{\sqrt{(x - x_i)^2 + (y - y_i)^2}}{\frac{2b}{a} + (z + z_i)} \tag{6}$$

and the angle of this straight line with respect to the horizontal axis can be expressed as

$$\theta_i = \arctan \frac{z - z_i}{\sqrt{(x - x_i)^2 + (y - y_i)^2}} \tag{7}$$

© 2026 by the author(s). Distributed under a Creative Commons CC BY license.

Preprints.org (www.preprints.org) | NOT PEER-REVIEWED | Posted: 28 April 2026 doi:10.20944/preprints202604.1929.v1

Above all, the actual ray traveling time (RTT) from the ith sensor to the target along the bent curve is formulated as

$$\hat{t}_i = \frac{1}{a}\left[\ln\left(\frac{1+\sin(\theta_i+\alpha_i)}{\cos(\theta_i+\alpha_i)}\right) - \ln\left(\frac{1+\sin(\theta_i-\alpha_i)}{\cos(\theta_i-\alpha_i)}\right)\right] \tag{8}$$

1.2. Problem Formulation

From the above definition, we can deduce the correlation between the observation performance of the sensors with respect to the target and the localization error. The CRLB establishes a fundamental limit for unbiased estimators in parameter estimation problem. Mathematically, the CRLB is defined as the inverse matrix of the FIM. Given an unbiased estimator for $\hat{\mathbf{u}}$ the parameter vector $\mathbf{u}$, the covariance matrix of $\hat{\mathbf{u}}$ is bounded from below by the CRLB, then we can obtain

$$E\left[(\hat{\mathbf{u}}-\mathbf{u})(\hat{\mathbf{u}}-\mathbf{u})^{\mathrm{T}}\right] \geq \mathbf{CRLB}(\mathbf{u}) = \mathbf{FIM}^{-1} \tag{9}$$

where **FIM** is defined as the inverse matrix of **CRLB**. The natural logarithm of the joint probability density function (PDF) of the localization measurement vector $\mathbf{t}$ and the target location estimation is derived as follows

$$\ln p(\mathbf{u};\mathbf{t}) = -\frac{1}{2}(\mathbf{t}-\hat{\mathbf{t}})^T\mathbf{Q}^{-1}(\mathbf{t}-\hat{\mathbf{t}}) \tag{10}$$

Owing to the spatial heterogeneity of the marine environment, the ambient noise variance and underwater sound speed exhibit significant depth-dependent variations. Accordingly, we denote the noise variance and sound speed associated with the ith sensor as σ_i, c_i, respectively. The corresponding **FIM** is given by

$$\mathbf{FIM} = \sum_{i=1}^{N}\begin{bmatrix} \frac{1}{c_i^2\sigma_i^2}\frac{(x-x_i)^2}{r_i^2} & \frac{1}{c_i^2\sigma_i^2}\frac{(x-x_i)(y-y_i)}{r_i^2} & \frac{1}{c_i^2\sigma_i^2}\frac{(x-x_i)(z-z_i)}{r_i^2} \\ \frac{1}{c_i^2\sigma_i^2}\frac{(x-x_i)(y-y_i)}{r_i^2} & \frac{1}{c_i^2\sigma_i^2}\frac{(y-y_i)^2}{r_i^2} & \frac{1}{c_i^2\sigma_i^2}\frac{(y-y_i)(z-z_i)}{r_i^2} \\ \frac{1}{c_i^2\sigma_i^2}\frac{(x-x_i)(z-z_i)}{r_i^2} & \frac{1}{c_i^2\sigma_i^2}\frac{(y-y_i)(z-z_i)}{r_i^2} & \frac{1}{c_i^2\sigma_i^2}\frac{(z-z_i)^2}{r_i^2} \end{bmatrix} \tag{11}$$

Thus, the trace of **CRLB** can be expressed as

$$T_{ar} = \frac{1}{\det(\mathbf{FIM})}\left[\left(\sum_{i=1}^{N}\frac{(z-z_i)}{c_i\sigma_i^2 r_i}\right)^2 - \left(\sum_{i=1}^{N}\frac{(x-x_i)}{c_i\sigma_i^2 r_i}\right)^2 - \left(\sum_{i=1}^{N}\frac{(y-y_i)}{c_i\sigma_i^2 r_i}\right)^2\right] \tag{12}$$

Given a narrowband acoustic signal characterized by a bandwidth of $B(\mathrm{Hz})$, a center frequency of $f_c(\mathrm{Hz})$, and a duration of $T_s(\mathrm{s})$, the theoretical **CRLB** for TOA estimation can be obtained [30]

$$\sigma_i^2 \geqslant \mathrm{CRLB(TOA)} = \frac{1}{8\pi^2 B T_s f_c^2 \mathrm{SNR}_i} \tag{13}$$

where SNR_i represent the received signal-to-noise ratio at the ith sensor. Based on the analysis of underwater acoustic channel characteristics, the received signal-to-noise ratio at each sensor can be calculated once the system operating parameters are determined.

According to the classical passive sonar equation, neglecting the directivity of the acoustic transducer, the signal-to-noise ratio at the ith sensor in UASNs is given by

$$\mathrm{SNR}_i^s = \mathrm{SL} - \mathrm{TL}_i - \mathrm{NL}_i \tag{14}$$

where SL represents the source level of the acoustic signal radiated by the target, TL_i denotes the propagation loss from the target to the ith receiving sensor, and NL_i corresponds to the ambient noise

© 2026 by the author(s). Distributed under a Creative Commons CC BY license.

Preprints.org (www.preprints.org) | NOT PEER-REVIEWED | Posted: 28 April 2026 doi:10.20944/preprints202604.1929.v1

ocean level at that sensor. Note that (14) is the decibel scale signal-to-noise ratio, which is converted to linear power signal-to-noise ratio as

$$\mathrm{SNR}_i^P = 10^{\mathrm{SNR}_i^s/10} \tag{15}$$

Substituting (14) and (15) into (13), the TOA estimation variance in the underwater environment is given by

$$\sigma_i^2 \geq \mathrm{CRLB}(\mathrm{TOA}) = \frac{1}{8\pi^2 B T_s f_c^2 \mathrm{SNR}_i^P} \tag{16}$$

It can be seen from (16) that the variance of TOA estimation is determined by the propagation loss and ambient noise in the marine environment.

2. Sensor Placement Solutions

In the preceding section, we first established the TOA measurement model for UASNs based on a realistic isogradient sound speed profile and actual ray traveling time. Subsequently, we systematically investigated the relationship between TOA estimation variance, propagation loss, ambient noise. Nevertheless, all the above analyses are predicated on the unrealistic assumption that the exact target location is known in advance, which is invalid in practical localization scenarios. To achieve consistent and superior localization performance over the entire test region, we adopt the optimization criterion of minimizing the trace of the average CRLB over all possible target locations. The corresponding objective function is formulated as

$$T_{AVG} = \frac{1}{\Omega} \iiint\limits_{\Omega} T_{ar} dxdydz \tag{17}$$

where Ω represents the test region, and T_{AVG} is defined as the trace of the average CRLB at all possible target positions within Ω. It should be noted that due to the nonlinearity of the underwater acoustic propagation model and the CRLB expression, the integral in the above (17) has no closed-form solution when substituting (12).

To facilitate numerical solution, we discretize the continuous test region into a uniform grid of candidate target locations. Under this discretization scheme, the corresponding optimization objective function for sensor placement can be rewritten as

$$\arg \min_{\mathbf{p}_1, \mathbf{p}_2, \cdots, \mathbf{p}_N} T_{AVG} = \arg \min_{\mathbf{p}_1, \mathbf{p}_2, \cdots, \mathbf{p}_N} \frac{1}{M} \sum_{M}^{m=1} \sqrt{T_{ar}(\mathbf{q}_m)} \tag{18}$$

where M denotes the total number of discrete target points, $\mathbf{q}_m$ is the mth target position in the test region, and the vector $\mathbf{p} = \left[p_{x,1}, p_{y,1}, p_{z,1}, p_{x,2}, p_{y,2}, p_{z,2}, \cdots, p_{x,N}, p_{y,N}, p_{z,N}\right]^{\mathrm{T}}$ is formed by concatenating the three-dimensional coordinates of all N underwater acoustic sensors. Given the non-convex nature of the optimization problem (18), we employ the MinMax k-Means optimization algorithm to find a suboptimal solution through iterative computation [31]. The detailed implementation steps of the algorithm are outlined below

1. **Initialization**
   The initial positions of N sensors are selected using the MinMax k-Means initialization strategy:
   - Randomly select a point in the test region Ω as the initial position of the first sensor $\mathbf{p}_1$,
   - Select the point in Ω farthest from $\mathbf{p}_1$ as the initial position of the second sensor $\mathbf{p}_2$,
   - For $i = 3 \cdots N$: selecting the point that maximizes the minimum Euclidean distance to all ready selected sensors.
2. **Iterative Optimization**
   The iterative framework is similar to the standard k-Means algorithm, but the update rule does not compute the centroid of each cluster. Instead, the position of each sensor is optimized individually to minimize the overall objective function. The detailed steps are as follows:

© 2026 by the author(s). Distributed under a Creative Commons CC BY license.

Preprints.org (www.preprints.org) | NOT PEER-REVIEWED | Posted: 28 April 2026 doi:10.20944/preprints202604.1929.v1

- **Allocation Step**: Assign each virtual target point $\mathbf{q}_m$ to its nearest sensor to form clusters:

$$\mathcal{C}_k^{(t)} = \left\{ \mathbf{q}_m : k = \arg\min_j \boldsymbol{\theta}_m - \mathbf{p}_j^{(t)} \right\}, \quad k = 1, \ldots, K \tag{19}$$

where $\mathcal{C}_k^{(t)}$ denotes the set of target points assigned to the k sensor at iteration t.
- **Update Step**: For each cluster, $k = 1, \ldots, K$, if $\left|\mathcal{C}_k^{(t)}\right| = 0$, randomly generate a new position in the test region. Otherwise, fix the positions of all other sensors and update the position of sensor $\mathbf{p}_k^{(t)}$ by solving the following sub-optimization problem numerically

$$\mathbf{p}_k^{(t+1)} = \arg\min_{\mathbf{p} \in \Omega} \sum_{\mathbf{q}_m \in \mathcal{C}_k^{(t)}} \mathrm{Tr}\left(\mathbf{CRLB}\left(\mathbf{q}_m; \mathbf{P}_{-k}^{(t)} \cup \{\mathbf{p}\}\right)\right) \tag{20}$$

with $\mathbf{P}_{-k}^{(t)} = \left\{\mathbf{p}_1^{(t)}, \ldots, \mathbf{p}_{k-1}^{(t)}, \mathbf{p}_{k+1}^{(t)}, \ldots, \mathbf{p}_K^{(t)}\right\}$

Mathematically, this update rule implements a block coordinate descent optimization scheme [32]. Specifically, we decompose the original high-dimensional optimization problem into N independent low-dimensional subproblems. For each subproblem, we fix the positions of all sensors except the j-th one, and adjust the position of the j-th sensor to minimize the sum of $\mathrm{tr}(\mathbf{CRLB})$ over all virtual target points assigned to that sensor.

3. **Convergence Judgment**
Terminate the iteration if the maximum position change of all sensors is less than a predefined threshold ϵ

$$\max_k \left\| \mathbf{p}_k^{(t+1)} - \mathbf{p}_k^{(t)} \right\| < \epsilon \tag{21}$$

4. **Output**
Return the optimized sensor placement matrix $\mathbf{P}^{(t+1)}$.

3. Simulation Studies

In this section, comprehensive simulations are carried out to evaluate the performance of the proposed sensor placement strategies for UASNs. Specifically, we first configure the simulation parameters, then employ the MinMax k-Means algorithm to optimize sensor placement in UASNs, and finally a systematic comparison of the root mean squared error (RMSE) performance is presented for three representative sensor placement strategies.

The simulation parameters are configured as follows. Bulleted lists look like this:

- **Signal Parameters**: The center frequency is set to $f_c = 1000$Hz, the sampling interval $T_s = 0.001$s, the bandwidth $B = 600$Hz, and the source level $SL = 180$dB. The ambient noise at each sensor is a random value in the interval of $60 - 70$dB.
- **Underwater Acoustic Propagation Parameters**: The depth range of the acoustic target is set to $0 - 1000$m. The distance between the target and each sensor ranges from 0m to 1500m, and the acoustic emission angle ranges from -90° to 90°. The surface sound speed is $b = 1480$m/s , and the underwater sound speed profile is assumed to be isogradient, increasing linearly with depth z as (5), and linear sound speed profile with steepness $a = 0.1$.
- **MinMax *k*-Means Algorithm Parameters**: The target location probability is uniformly distributed in the test region. The region is discretized into a regular grid with a spacing of 10m, where each grid intersection is treated as a virtual target point. The algorithm is terminated when the maximum number of iterations $t = 1000$ is reached or the convergence condition $\varepsilon = 0.01$ is satisfied.

In a 1000m $\times$ 1000m $\times$ 1000m test region, the MinMax k-Means algorithm is employed to optimize the sensor placement under the assumption of uniform target occurrence probability. All algorithmic

© 2026 by the author(s). Distributed under a Creative Commons CC BY license.

Preprints.org (www.preprints.org) | NOT PEER-REVIEWED | Posted: 28 April 2026 doi:10.20944/preprints202604.1929.v1

parameters are set in accordance with the configurations given above. The surveillance region is discretized into a 3D grid with a spacing of 10m, where each grid intersection is regarded as a virtual target point. Simulations are performed with the number of sensors set to 5, 10, 20, and 30, respectively. The optimal sensor placement for UASNs obtained by the proposed algorithm is illustrated in Figure 1.

Figure 1 presents the optimal sensor placement results obtained by the MinMax *k*-Means algorithm with different numbers of sensors, where the distribution of sensors and virtual target points varies with the number of sensors. It can be observed from Figure 1(a) to (d) that the number of sensors increases gradually. Specifically, Figure 1(a) exhibits 5 sensors with a sparse yet approximately uniform distribution within the test region. As the number of sensors increases stepwise in Figure 1(b) and (c), the sensors are distributed more extensively and uniformly across the entire region. In Figure 1(d), the spatial distribution of sensors becomes further homogenized, which ensures more thorough coverage of the surveillance region and effectively covers all virtual target points.

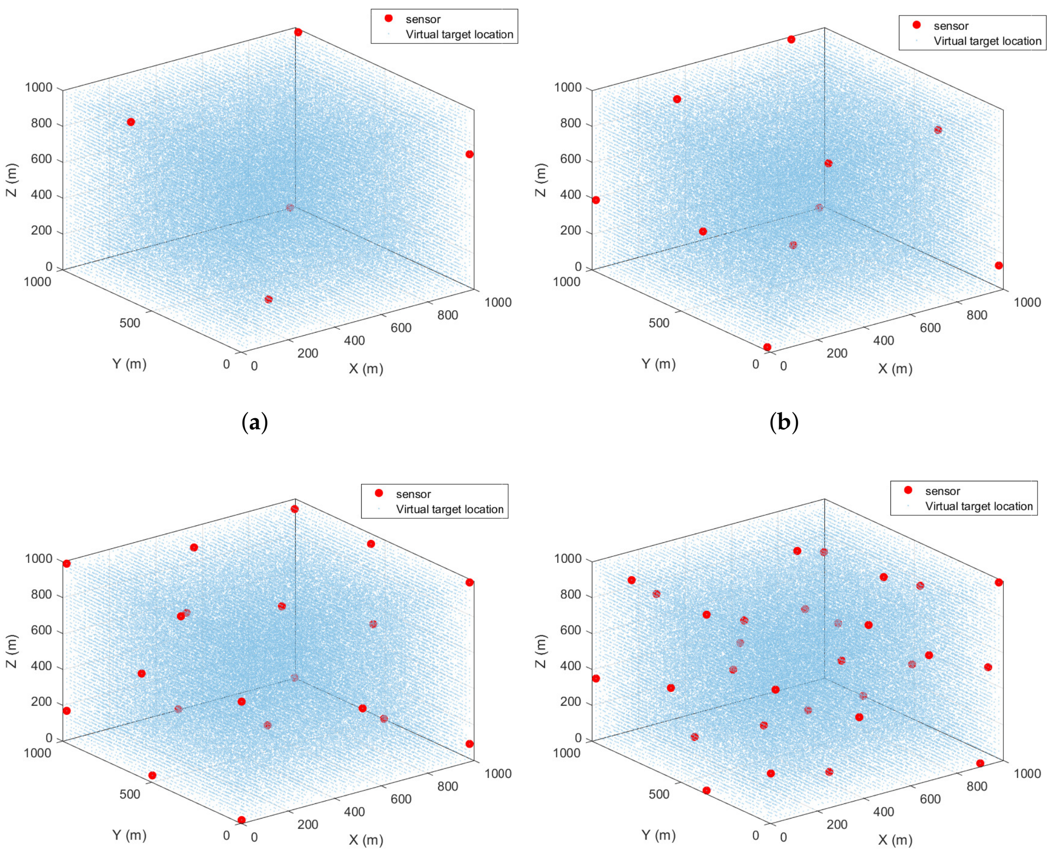

(a) (b) (c) (d)

Figure 1. The optimal sensor placements are carried out by taking the number of sensors with N, they should be listed as: (**a**)$N = 5$. (**b**) $N = 10$. (**c**) $N = 20$. (**d**) $N = 30$.

These results demonstrate that the optimized placeyment positions obtained via the MinMax *k*-Means algorithm present an approximately uniform distribution in the test region for different numbers of sensors, which well satisfies the requirements for accurate localization of virtual target points.

In the follows, we evaluate the localization performance of the proposed placement strategies by comparing its localization accuracy with two typical benchmark methods, namely, random placement

© 2026 by the author(s). Distributed under a Creative Commons CC BY license.

Preprints.org (www.preprints.org) | NOT PEER-REVIEWED | Posted: 28 April 2026 doi:10.20944/preprints202604.1929.v1

and cube placement. To quantitatively assess the localization performance, the RMSE between the actual target positions and their estimated positions is calculated as follows

$$\text{RMSE}=\sqrt{\mathbb{E}\left\{\|\hat{\mathbf{q}}-\mathbf{q}\|^2\right\}} \tag{22}$$

Figure 2 presents a comparison of the RMSE versus the number of sensors for three different sensor placement stratagies. As observed in Figure 2, while the RMSE curves of all three placement schemes exhibit a decreasing trend with an increasing number of sensors, the proposed MinMax k-Means scheme outperforms the other two methods by consistently achieving the lowest localization error. A key advantage of the proposed method is that it not only achieves an approximately uniform spatial distribution of sensors but also incorporates the inherent characteristics of the marine environment into the placement optimization process. This unique combination of features makes the proposed algorithm more robust and suitable for practical applications in UASNs.

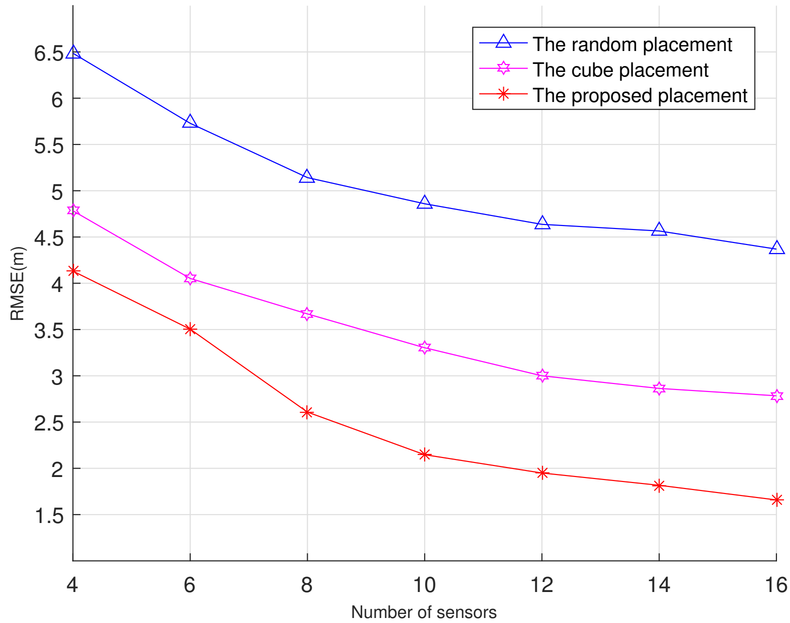

Figure 2. Comparison of RMSEs versus number of sensors among three different placements with the steepness of SSP is a=0.1

Furthermore, we conduct a systematic investigation into the influence of critical environmental parameters on the performance of the proposed MinMax k-Means algorithm, with the corresponding experimental results depicted in Figure 3 and Figure 4. Specifically, Figure 3 presents a quantitative analysis of the RMSE for the three placement schemes as a function of the ToA estimation variance σ_i^2.

For this set of simulations, the number of placed sensors is fixed at $N = 8$, and the noise variance is varied in the range of $0.1m^2$ to $1m^2$. As clearly observed from the figure, the RMSE values of all three placement strategies increase linearly with the growth of σ_i^2, while the proposed method maintains a consistently lower RMSE and outperforms the other two schemes in terms of estimation performace. Importantly, the proposed algorithm retains its superior localization performance even when subjected to large measurement noise, demonstrating its robustness to noise perturbations.

© 2026 by the author(s). Distributed under a Creative Commons CC BY license.

Preprints.org (www.preprints.org) | NOT PEER-REVIEWED | Posted: 28 April 2026
doi:10.20944/preprints202604.1929.v1

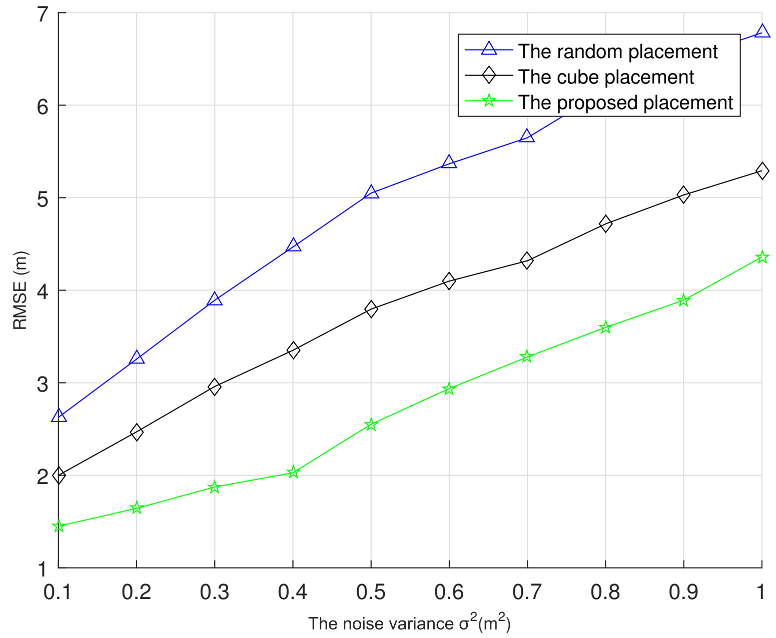

Figure 3. Impacts of the noise variance on the localization performance under different placements with $N = 8$.

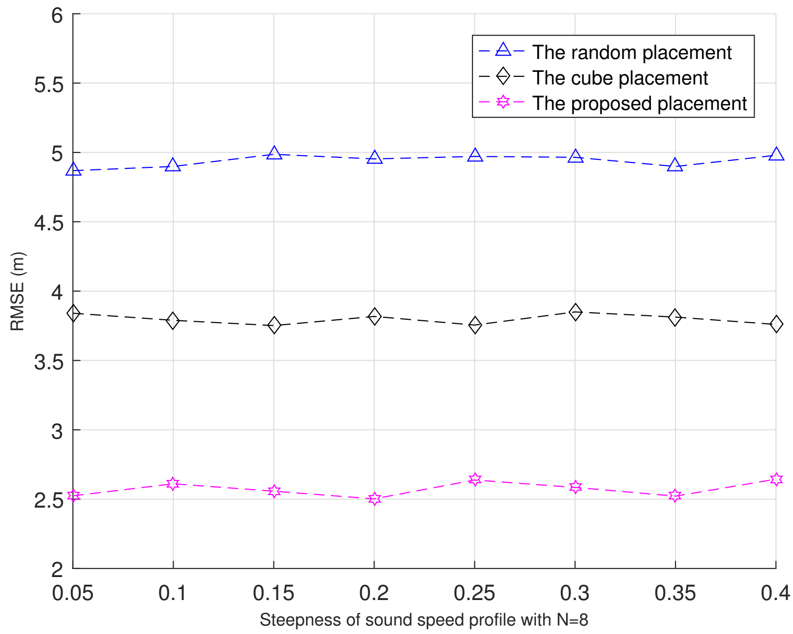

Figure 4. Impacts of the steepness of the SSP on the localization performance for different deployments with $N = 8$.

Additionally, Figure 4 evaluates the impact of the SSP steepness on the localization performance of the three placement strategies. It is evident that the RMSE curve of the proposed algorithm exhibits the least fluctuation when the SSP steepness changes, indicating its strong adaptability to variations in the underwater sound speed profile. Furthermore, across the entire range of SSP steepness values, the proposed algorithm consistently achieves superior localization performance compared to the other two placement strategies. Collectively, the simulation results validate that the MinMax *k*-Means placement strategy offers optimal localization performance and enhanced robustness, making it well-suited for application in dynamically changing underwater acoustic environments.

© 2026 by the author(s). Distributed under a Creative Commons CC BY license.

Preprints.org (www.preprints.org) | NOT PEER-REVIEWED | Posted: 28 April 2026 doi:10.20944/preprints202604.1929.v1

4. Conclusions

In this paper, the optimal sensor placement problem for 3-D TOA-based localization in UASNs is considered. A localization measurement model with varied noise measurements and a realistic isogradient SSP is proposed, and the trace of the average CRLB is used as the optimization criterion. Additionally, the MinMax k-Means algorithm is employed to solve the optimal sensor placement problem by minimizing the average of the trace of CRLB. Simulation results show that the proposed method achieves better localization accuracy while maintaining satisfactory localization performance in an underwater environment with dynamic changes.

In future research, we will extend our work to the the scenario of multiple uncertain targets with distinct probability distributions, as this scenario is more consistent with the practical requirements of underwater surveillance applications. Furthermore, we will explore the sensor placement problem for uncertain moving targets in UASNs, aiming to develop a more flexible and practical placement strategy that can adapt to the dynamic nature of underwater targets.

Author Contributions: Conceptualization, Z.R. and M.L.; methodology, Z.R.; validation, Z.R. and W.T.; writing—original draft preparation, Z.R.; writing—review and editing, Z.R., M.L. and B.W.; supervision, W.T.; funding acquisition, W.T. and Z.R. All authors have read and agreed to the published version of the manuscript.

Funding: This research was funded by the National Natural Science Foundation of China under Grant 62361010, and the Foundation of Henan Provincial Department of Science and Technology under Grant 242102211015

Conflicts of Interest: The authors declare no conflict of interest.

References

1. Erol-Kantarci, M.; Mouftah, H.T.; Oktug, S. A Survey of Architectures and Localization Techniques for Underwater Acoustic Sensor Networks. *IEEE Commun. Surv. Tutor.* **2011**, *13*, 487–502. doi:10.1109/surv.2011.020211.00035.
2. Yan, J.; Guo, D.; Luo, X.; Guan, X. AUV-Aided Localization for Underwater Acoustic Sensor Networks With Current Field Estimation. *IEEE Trans. Veh. Technol.* **2020**, *69*, 8855–8870. doi:10.1109/TVT.2020.2996513.
3. Wang, K.; Gao, H.; Xu, X.; Jiang, J.; Yue, D. An Energy-Efficient Reliable Data Transmission Scheme for Complex Environmental Monitoring in Underwater Acoustic Sensor Networks. *IEEE Sens. J.* **2016**, *16*, 4071–4082. doi:10.1109/jsen.2015.2428712.
4. Lei, Z.; Lei, X.; Na, W.; Zhang, Q. Present status and challenges of underwater acoustic target recognition technology: A review. *Front. Phys.* **2022**. doi:10.3389/fphy.2022.1044890.
5. Su, X.; Ullah, I.; Liu, X.; Choi, D. A Review of Underwater Localization Techniques, Algorithms, and Challenges. *J. Sensors* **2020**, 6403161. doi:10.1155/2020/6403161.
6. Zou, Y.; Fan, J. Source Localization Using TDOA Measurements From Underwater Acoustic Sensor Networks. *IEEE Sens. Lett.* **2023**, *7*, 1–4. doi:10.1109/LSENS.2023.3274200.
7. Kim, J. 3-D Localization of Heterogeneous Underwater Networks Using Hybrid TOA-AOA Measurements Under Random DoS Attack. *IEEE IoT J.* **2025**, *12*, 22257–22266. doi:10.1109/JIOT.2025.3550398.
8. Han, G.; Jiang, J.; Shu, L.; Xu, Y.; Wang, F. Localization Algorithms of Underwater Wireless Sensor Networks: A Survey. *Sensors* **2012**, *12*, 2026–2061. doi:10.3390/s120202026.
9. Toky, A.; Singh, R. P.; Das, S. Localization schemes for Underwater Acoustic Sensor Networks - A Review. *Comput. Sci. Rev.* **2020**, 100241. doi:10.1016/j.cosrev.2020.100241.
10. Yan, J.; Guan, X.; Yang, X.; Chen, C.; Luo, X. A Survey on Integration Design of Localization, Communication, and Control for Underwater Acoustic Sensor Networks. *IEEE Internet Things J.* **2025**, *12*, 6300–6324. doi:10.1109/JIOT.2025.275284766.
11. Zhang, R. Three-dimensional positioning based on TOA combining acoustic signal and optical signal. *Front. Comput. Intell. Syst.* **2023**, *1*, 12–19. doi:10.1234/fcis.2023.257789279.
12. Jiang, F.; Zhang, Z. An improved underwater TDOA/AOA joint localisation algorithm. *IET Commun.* **2021**, *15*, 802–814. doi:10.1049/cmu2.12145.
13. Sun, D.; Zhang, P.; Cai, K. Joint Estimation of Underwater Target Location and Sound Speed Profile Based on Argo Data. *IEEE IoT J.* **2025**, *12*, 17110–17122. doi:10.1109/JIOT.2025.3537972.

© 2026 by the author(s). Distributed under a Creative Commons CC BY license.

Preprints.org (www.preprints.org) | NOT PEER-REVIEWED | Posted: 28 April 2026 doi:10.20944/preprints202604.1929.v1

14. Tuna, G.; Gungor, V.C. A survey on deployment techniques, localization algorithms, and research challenges for underwater acoustic sensor networks. *Int. J. Commun. Syst.* **2017**, *30*, e3350. doi:10.1002/dac.3350.
15. Kim, J. Optimal Hydrophone Placement Method of Bistatic Sonar Sensors for Tracking Underwater Targets. *IEEE IoT J.* **2025**, *12*, 29758–29765. doi:10.1109/JIOT.2025.3568820.
16. Bishop, A.N.; Fidan, B.; Anderson, B.D.O.; Dogancay, K.; Pathirana, P.N. Optimality analysis of sensor-target localization geometries. *Automatica* **2010**, *46*, 479–492. doi:10.1016/j.automatica.2009.12.003.
17. Mei, X.; Han, D.; Saeed, N.; Wu, H.; Han, B.; Li, K.C. Localization in Underwater Acoustic IoT Networks: Dealing With Perturbed Anchors and Stratification. *IEEE Internet Things J.* **2024**, *11*, 17757–17769. doi:10.1109/JIOT.2024.268015737.
18. Xu, S.; Wu, L.; Doğançay, K.; Shankar, M. R. B.; Ho, K. C.; Wu, X. Optimal Sensor Placement for Target Localization in IoT Systems: A Cramér-Rao Bound Perspective. *IEEE IoT Mag.* **2025**, *8*, 120–126. doi:10.1109/MIOT.2025.3575317.
19. Nguyen, N.H.; Doğançay, K. Optimal Geometry Analysis for Multistatic TOA Localization. *IEEE Trans. Signal Process.* **2016**, *64*, 4180–4193. doi:10.1109/tsp.2016.2566611.
20. Xu, S.; Ou, Y.; Wu, X. Optimal Sensor Placement for 3-D Time-of-Arrival Target Localization. *IEEE Trans. Signal Process.* **2019**, *67*, 4928–4942. doi:10.1109/tsp.2019.2932872.
21. Fang, X.; He, Z.; Shi, R. Optimality analysis of range sensor placement under constrained deployment region. *Wirel. Netw.* **2023**, *29*, 3309–3321. doi:10.1007/s11276-023-03357-x.
22. Aubry, A.; Babu, P.; Braca, P.; Maio, A.D.; Panwar, K. Sensor Placement Strategies for Target Localization via 3-D AOA Measurements. *IEEE Trans. Aerosp. Electron. Syst.* **2025**, *61*, 2134-2148. doi:10.1109/TAES.2024.3463636.
23. Gola, K. K.; Gupta, B. Underwater sensor networks: Comparative analysis on applications, deployment and routing techniques. *IET Commun.* **2020**. doi:10.1049/iet-com.2019.1171.
24. Chaudhary, M.; Goyal, N.; Benslimane, A.; Awasthi, L.K.; Alwadain, A.; Singh, A. Underwater Wireless Sensor Networks: Enabling Technologies for Node Deployment and Data Collection Challenges. *IEEE Internet Things J.* **2023**, *10*, 7020–7041. doi:10.1109/jiot.2022.3218766.
25. Moreno-Salinas, D.; Pascoal, A.M.; Aranda, J. Optimal Sensor Placement for Acoustic Underwater Target Positioning With Range-Only Measurements. *IEEE J. Ocean. Eng.* **2016**, *41*, 620–643. doi:10.1109/joe.2015.2494918.
26. Zhang, Y.; Li, Y.; Zhang, Y.; Jiang, T. Underwater Anchor-AUV Localization Geometries With an Isogradient Sound Speed Profile: A CRLB-Based Optimality Analysis. *IEEE Trans. Wirel. Commun.* **2018**, *17*, 8227–8238. doi:10.1109/twc.2018.2875432.
27. Huang, W.; Qiu, R.; Zhou, J.; Xu, T. Deployment Strategy Analysis for Underwater Geodetic Networks. *J. Mar. Sci. Eng.* **2023**, *12*, 25. doi:10.3390/jmse12010025.
28. Huang, W.; Wu, P.; Xu, T.; Zhang, H.; Meng, K. Optimal Reference Nodes Deployment for Positioning Seafloor Anchor Nodes in the Internet of Underwater Things. *IEEE Internet Things J.* **2024**, *11*, 1–12. doi:10.1109/jiot.2024.3524405.
29. Ramezani, H.; Rad, H.J.; Leus, G. Target Localization and Tracking for an Isogradient Sound Speed Profile. *IEEE Trans. Signal Process.* **2013**, *61*, 1434–1446. doi:10.1109/tsp.2012.2235432.
30. Saric, Z.; Kukolj, D.; Teslic, N. Acoustic Source Localization in Wireless Sensor Network. *Circuits Syst. Signal Process.* **2010**, *29*, 837–856. doi:10.1007/s00034-010-9187-3.
31. Tzortzis, G.; Likas, A. The MinMax k-Means clustering algorithm. *Pattern Recognit.* **2014**, *47*, 2505–2516. doi:10.1016/j.patcog.2014.01.015.
32. Nie, F.; Li, Z.; Wang, R.; Li, X. An Effective and Efficient Algorithm for K-Means Clustering With New Formulation. *IEEE Trans. Knowl. Data Eng.* **2023**. doi:10.1109/TKDE.2022.3155450.

Disclaimer/Publisher's Note: The statements, opinions and data contained in all publications are solely those of the individual author(s) and contributor(s) and not of MDPI and/or the editor(s). MDPI and/or the editor(s) disclaim responsibility for any injury to people or property resulting from any ideas, methods, instructions or products referred to in the content.

© 2026 by the author(s). Distributed under a Creative Commons CC BY license.